

INSTITUT FÜR KERNPHYSIK, UNIVERSITÄT FRANKFURT
D - 60486 Frankfurt, August-Euler-Strasse 6, Germany

IKF-HENPG/2-98

On the Early Stage of Nucleus–Nucleus Collisions

Marek Gaździcki¹

Institut für Kernphysik, Universität Frankfurt, Germany

Mark I. Gorenstein^{2,3}

Institute for Theoretical Physics, University of Frankfurt, Germany

and

School of Physics and Astronomy, Tel Aviv University, Israel

A statistical model of the early stage of central nucleus–nucleus collisions is developed and confronted with the experimental data. The analysis leads to the conclusion that a Quark Gluon Plasma is created in central nucleus–nucleus collisions at the SPS. The localization and the properties of the transition region are discussed. It is shown that the transition can be detected by observation of the characteristic behaviour of pion and strangeness multiplicities, and an increase of the event–by–event fluctuations. An attempt to understand the data on J/Ψ production in Pb+Pb collisions at SPS within the same approach is presented.

We are surprised by the success of the statistical approach to the early stage of nucleus–nucleus collisions in describing the results on pion, strangeness and J/Ψ production.

February 5, 2020

¹E-mail: marek@ikf.physik.uni-frankfurt.de

²Permanent address: Bogolyubov Institute for Theoretical Physics, Kiev, Ukraine

³E-mail: goren@th.physik.uni-frankfurt.de

1 Introduction

At the final state of high energy nuclear collisions many new particles appear. They are massive and extended objects: hadrons and hadronic resonances. What is the nature of particle creation in strong interactions? How does matter look like in a state of very high energy density which is created during the collision of two nuclei? These questions motivate a broad experimental programme in which properties of high energy nuclear collisions are investigated [1].

Due to a lack of a calculable theory of strong interaction the interpretation of the experimental results has to rely on phenomenological approaches. The first proposed models of high energy collision process were statistical models of the early stage [2, 3], the stage in which excitation of the incoming matter takes place. In their original formulations the models failed to reproduce experimental results. However, when the broad set of the data became available [4, 5], it was realized [6, 7] that after necessary generalization a statistical approach to the early stage gives surprising agreement with the results. It could be therefore used as a tool to identify the properties of the state created at the early stage. The aim of this paper is further development of the statistical model of the early stage and its application to study the properties of the high energy density state created in nucleus–nucleus collisions.

A special role in this study is played by the entropy [8] (at high collision energy carried mainly by final state pions) and heavy flavours (strangeness, charm) production [9, 10, 11]. It can be argued that they are insensitive to the late stages of the collision and therefore they carry information on the early stage.

The form of the strongly interacting matter at very high energy density is theoretically well established in terms of perturbative QCD, which is in agreement with lattice QCD simulations at zero baryonic density. At high temperatures lattice QCD predicts a quasi-ideal gas of deconfined quarks and gluons called Quark Gluon Plasma (QGP) [12]. When this form of matter is assumed in the statistical model of the early stage, the results on strangeness and pion production in nucleus–nucleus collisions at the SPS are reproduced in an essentially parameter free way [7].

This surprising agreement should be contrasted with the problems [13, 14] of microscopic non-equilibrium models in describing the same set of data. Scaling properties of the data, natural in the thermodynamical approach, arise in non-equilibrium models as an accidental cancelation of many non-scaling dependences.

All that motivates further development of the experimental programme [15]. The main goal is to localize the collision energy region in which the deconfinement transition takes place and study the properties of the transition itself. In this region many anomalies are expected. Their experimental observation will lead us to definite conclusion concerning the early stage of nucleus–nucleus collisions. The corresponding experimental study at the SPS should start in 1999 when beams of lower than maximal SPS energy will become available. The experiments NA49 [15] and NA54 are now being prepared for this investigation.

The main goal of this paper is a development of the statistical model of the early stage in order to provide a description of the transition region, with special attention paid to the observables which can be measured in the experimental programme. This can

be done only when the partition function of the confined matter state is also given. We argue that this state should not be modeled as a gas of hadrons and hadronic resonances. Consequently we have to introduce an effective parametrization of the confined state and try to extract its properties from the comparison with the experimental data.

Finally we attempt to include in the analysis a production of charm and existing experimental data on J/Ψ production [16]. The standard approach is a hard QCD J/Ψ creation and its further partial suppression in the surrounding matter. This approach leads to the conclusion [17] of creation of the QGP only in central Pb+Pb collisions at SPS, but not in the collisions of lighter nuclei. Pion and strangeness data show however no essential difference between central S+S and Pb+Pb collisions at SPS. They are consistent within statistical model analysis with creation of the QGP already in central S+S collisions at SPS. Thus the crucial question is to what extent is this contradiction caused by the use of different approaches for data interpretation? Can consistent data description, including production of charm, be obtained using the statistical approach?

The paper is organized as follows. The model used further for data interpretation and analysis of the transition region is defined in Section 2. The basic features of the model are presented in Section 3, where the approximate analytical formulae are given together with the numerical results obtained using the full version of the model. The model is confronted with the experimental data in Section 4. In Section 5 the discussion of the different approaches to the strangeness and J/Ψ production is given. Summary and conclusions close the paper.

For simplicity reasons we consider only central collisions of two identical nuclei (central A+A collisions). The nuclear mass number is denoted by A . The whole discussion is done in the center of mass system. The c.m. energy of nucleon–nucleon pair and nucleon mass are denoted by \sqrt{s}_{NN} and m_N , respectively.

2 A Model of the Early Stage of A+A Collisions

1. The basic assumption of our model is that the production of new particles in the early stage of nucleus–nucleus collisions is a statistical process. Thus formation of all microscopic states allowed by conservation laws is equally probable. This means that the probability to produce a given macroscopic state is proportional to the total number of its microscopic realizations, i.e. a macroscopic state probability P is

$$P \sim e^S, \quad (1)$$

where S is the entropy of the macroscopic state.

2. As the particle creation process does not produce net baryonic, flavour and electric charges only states with the total baryon, flavour and electric numbers equal to zero should be considered. Thus the properties of the created state are entirely defined by the volume in which production takes place, the available energy and a partition function. In the case of collisions of large nuclei the thermodynamical approximation can be used and the dependence on the volume and the energy reduces to the dependence on the energy density. The state properties can be given in the form of a equation of state.

3. We assume that the early stage entropy creation takes place in the volume equal to the volume of the Lorentz contracted nucleus:

$$V = \frac{V_0}{\gamma}, \quad (2)$$

where $V_0 = 4/3\pi r_0^3 A$ and $\gamma = \sqrt{s_{NN}}/(2m_N)$. The r_0 parameter is taken to be 1.30 fm in order to fit the mean baryon density in the nucleus, $\rho_0 = 0.11 \text{ fm}^{-3}$.

4. Only a fraction of the total energy in A+A collision is transformed into the energy of created particles. This is because a part of the energy is carried by the conserved during the collision net baryon number. This available energy can be expressed as:

$$E = \eta(\sqrt{s_{NN}} - m_N) A, \quad (3)$$

The parameter η is assumed to be independent of the collision energy and the system size as suggested by the experimental data. This experimental observation is usually justified by a model of a quark–gluon structure of the nucleon [18]. The value of η used for the numerical calculations is 0.67 (see Section 4 for details).

5. In order to predict a probability of creation of a given macroscopic state all possible degrees of freedom and interaction between them should be given in the form of the partition function. In the case of large enough volume the grand canonical approximation can be used and the state properties can be given in the form of an equation of state. The question of how one can use this equation of state to calculate the space–time evolution (hydrodynamics) of the created system requires a special separate study.

6. The most elementary particles of strong interaction are quarks and gluons. In the following we consider u , d and s quarks and the corresponding antiquarks with the internal number of degrees of freedom equal to 6 (3 colour states \times 2 spin states). In the entropy

evaluation the contribution of c , b and t quarks can be neglected due to their large masses. The charm production is discussed separately in Section 5. The internal number of degrees of freedom for gluons is 16 (8 colour states \times 2 spin states). The masses of gluons and nonstrange (anti)quarks are taken to be 0, the strange (anti)quark mass is taken to be 175 MeV [19].

7. In the case of creation of colour quarks and gluons the equation of state is assumed to be the ideal gas equation of state modified by the bag constant B in order to account for a strong interaction between quarks and gluons and the surrounding QCD vacuum (see e.g. [20]):

$$p = p^{id} - B, \quad \varepsilon = \varepsilon^{id} + B, \quad (4)$$

where p and ε denote pressure and energy density, respectively, and B is the so called bag constant. The equilibrium state defined above is called Quark Gluon Plasma or Q-state.

8. At the final freeze-out stage of the collision the degrees of freedom are hadrons – extended and massive objects composed of (anti)quarks and gluons. Due to their finite proper volume hadrons can exist in their well defined asymptotic states only at rather low energy density. Estimates $\epsilon < 0.1 \div 0.4$ GeV/fm³ for the hadron gas with van der Waals excluded volume have been found in Ref. [21]. In the early stage of A+A collisions such a low energy density states could be created only at very low collision energies of a few GeV per nucleon. Asymptotic hadronic states can be questioned as a possible degrees of freedom in the early stage also on the base of our current understanding of $e^+ + e^-$ annihilation process, where the initial degrees of freedom are found to be colourless $q\bar{q}$ pairs [22].

Guided by this considerations we assume that at collision energies lower than the energy needed for a QGP creation the early stage effective degrees of freedom can be approximated by point-like colourless bosons. This state is called W-state (White state). The nonstrange degrees of freedom which dominate the entropy production are taken to be massless, as seems to be suggested by the original analysis of the entropy production in N+N and A+A collisions [6]. Their internal number of degrees of freedom was fitted to the same data [6, 7] to be about 3 times lower than the internal number of effective degrees of freedom for the QGP ($16 + (7/8) \cdot 36 \cong 48$). Thus it is taken to be $48/3 = 16$. The mass of strange degrees of freedom is assumed to be 500 MeV, equal to the kaon mass. The internal number of strange degrees of freedom is estimated to be 14 as extracted from the fit to the strangeness data at AGS (see Section 4). The phenomenological reduction factor 3 is used in our numerical calculations between the total number of degrees of freedom for Q-state and nonstrange W-state because of the different magnitude of strangeness suppression due to different masses of strangeness carriers in both cases. The ideal gas equation of state is selected. In Appendix A we discuss a possible interpretation of the degrees of freedom in W-state.

9. For large enough volume the grand canonical approximation can be used and the calculation of the entropy is significantly simplified. In a large system only one macroscopic state is produced – the state with the maximum entropy density, s . This is because the

relative probability of the state with the entropy density $s' < s$ is given by:

$$\frac{P}{P_{MAX}} = \exp [V (s' - s)] . \quad (5)$$

Thus the relative probability decreases to zero when the volume increases to infinity for any value of $s' < s$.

10. In the case of finite (small) volume the conservation laws should be accounted for in the strict way (canonical or microcanonical treatment). The macroscopic states with an entropy density lower than the maximum one are created with final probabilities. As the physical properties of various states can be significantly different (see Section 3) sizeable nontrivial event-by-event fluctuations are expected.

11. The maximum entropy state is called equilibrium state. In the model with two different states (W and Q) the form of the maximum entropy state changes with the collision energy. The regions, in which equilibrium state is in the form of pure W or pure Q state, are separated by the region in which both states coexist (mixed phase or W-Q-state).

12. It is important to note that the formation of state in global equilibrium in the early stage of nuclear collisions is a consequence of our basic assumption that all possible microscopic states are created with equal probability. Thus it is due to the assumed statistical nature of the primary creation process and it is not due to equilibration by a long lasting sequence of secondary interactions.

13. Globally equilibrated state created in the early stage expands and finally freezes-out in the form of hadrons and hadronic resonances. It was recently found that this hadronization process can be described by a statistical model [23, 24]. Thus phase-space seems to govern not only production of entropy and flavour content of the state in the early stage, as discussed in this paper, but also their conversion to hadrons which happens at a significantly lower energy scale.

14. Due to the Lorentz contraction along the collision axis the shape of the early stage volume is non-spherical. This causes that the isotropic angular distribution of particles in the early stage is converted during an anisotropic expansion into a forward-backward peaked distribution as observed in the experimental data.

15. We assume that the only process which changes the entropy content of the produced matter during the expansion, hadronization and freeze-out is an equilibration with the baryonic subsystem. It was argued that it leads to entropy transfer to baryons which corresponds to the effective absorption of about 0.35 π -mesons per baryon [6, 25]. This interaction causes also that the produced hadrons in the final state do not obey symmetries of the early stage production process, i.e. there are non-zero baryonic number and electric charge in the final hadron state.

16. It is assumed that the total number of s and \bar{s} quarks is conserved during the expansion, hadronization and freeze-out.

3 Calculations

In the first part of this section we analyze the simplified version of the model which allows us to perform calculations in an analytical way. The results of the numerical calculations done within the full version of the model are presented in the second part of the section.

The entropy calculation can be most easily done in the grand canonical formulation which is justified for large enough systems. As we consider the system with zero conserved charges the temperature T remains the only independent thermodynamical variable in the thermodynamical limit when the system volume goes to infinity. All chemical potentials in the system should be equal to zero. The system equation of state is convenient to define in terms of the pressure function $p = p(T)$ as the entropy and energy densities can be calculated from the thermodynamical relations:

$$s(T) = \frac{dp}{dT}, \quad \varepsilon(T) = T \frac{dp}{dT} - p. \quad (6)$$

For particle of species ‘ i ’ the ideal gas pressure is

$$p_i(T) = \frac{g_i}{2\pi^2} \int_0^\infty k^2 dk \frac{k^2}{3(k^2 + m_i^2)^{1/2}} \frac{1}{\exp\left(\frac{\sqrt{k^2 + m_i^2}}{T}\right) \pm 1}, \quad (7)$$

where g_i is the internal number of degrees of freedom (degeneracy factor) for i -th species, m_i is particle mass, ‘ -1 ’ appears in Eq. (7) for bosons and ‘ $+1$ ’ for fermions. The pressure $p(T)$ for the ideal gas of several particle species is additive: $p(T) = \sum_i p_i(T)$. The same is valid for the entropy and energy densities (6).

3.1 Analitical Calculations

In order to perform the analitical calculations of the system entropy and illustrate the model properties we simplify our consideration assuming that all degrees of freedom are massless. The momentum integral in Eq. (7) is easily calculated for $m_i = 0$:

$$p_i(T) = \frac{\sigma_i}{3} T^4, \quad (8)$$

where σ_i is the so called Stephan–Boltzmann constant, equal to $\pi^2 g_i/30$ for bosons and $\frac{7}{8}\pi^2 g_i/30$ for fermions. The total pressure in the ideal gas of several massless species can be presented then as $p(T) = \pi^2 g T^4/90$ with the effective number of degrees of freedom g given by

$$g = g_b + \frac{7}{8} g_f \quad (9)$$

in terms of degrees of freedom of all bosons g_b and all fermions g_f . It is taken to be g_W for W-state and g_Q for Q-state, with $g_Q > g_W$.

The model equation of state is presented then as

$$p_W(T) = \frac{\pi^2 g_W}{90} T^4, \quad \varepsilon_W(T) = \frac{\pi^2 g_W}{30} T^4, \quad s_W(T) = \frac{2\pi^2 g_W}{45} T^3, \quad (10)$$

$$p_Q(T) = \frac{\pi^2 g_Q}{90} T^4 - B, \quad \varepsilon_Q(T) = \frac{\pi^2 g_Q}{30} T^4 + B, \quad s_Q(T) = \frac{2\pi^2 g_Q}{45} T^3, \quad (11)$$

for the pure W- and Q-state, respectively. Note the presence of the non-perturbative bag terms in addition to the ideal quark-gluon gas expressions for the pressure and energy density of the Q-state.

The 1-st order phase transition between W- and Q-state is defined by the Gibbs criterion

$$p_W(T_c) = p_Q(T_c), \quad (12)$$

from which the phase transition temperature is calculated:

$$T_c = \left[\frac{90B}{\pi^2(g_Q - g_W)} \right]^{1/4}. \quad (13)$$

At $T = T_c$ the system is in the *mixed* phase with

$$\varepsilon_{mix} = (1 - \xi)\varepsilon_W^c + \xi\varepsilon_Q^c, \quad s_{mix} = (1 - \xi)s_W^c + \xi s_Q^c, \quad (14)$$

where $(1 - \xi)$ and ξ are the relative volumes occupied by the W- and Q-state, respectively. From Eqs. (10,11) one finds the energy density discontinuity ('latent heat')

$$\Delta\varepsilon \equiv \varepsilon_Q(T_c) - \varepsilon_W(T_c) \equiv \varepsilon_Q^c - \varepsilon_W^c = 4B. \quad (15)$$

From Eqs. (3,2) we find that the early stage energy density is given by:

$$\varepsilon \equiv \frac{E}{V} = \frac{\eta \rho_0 (\sqrt{s_{NN}} - 2m_N) \sqrt{s_{NN}}}{2m_N}. \quad (16)$$

For $\varepsilon < \varepsilon_W^c$ and $\varepsilon > \varepsilon_Q^c$ the system consists of pure W- and Q-state, respectively, with entropy density given by the following equations:

$$s_W(\varepsilon) = \frac{4}{3} \left(\frac{\pi^2 g_W}{30} \right)^{1/4} \varepsilon^{3/4}, \quad (17)$$

$$s_Q(\varepsilon) = \frac{4}{3} \left(\frac{\pi^2 g_Q}{30} \right)^{1/4} (\varepsilon - B)^{3/4}. \quad (18)$$

For $\varepsilon_W^c < \varepsilon < \varepsilon_Q^c$ the system is in the mixed phase (14) and its entropy density can be represented in the form

$$s_{mix}(\varepsilon) = \frac{\varepsilon_Q^c s_W^c - \varepsilon_W^c s_Q^c}{4B} + \frac{s_Q^c - s_W^c}{4B} \varepsilon \equiv a + b \varepsilon. \quad (19)$$

According to our basic assumptions in Section 2 the created macroscopic state should be defined by the entropy density maximum condition:

$$s(\varepsilon) = \max \{ s_W(\varepsilon), s_Q(\varepsilon), s_{mix}(\varepsilon) \}. \quad (20)$$

In Appendix B we prove a remarkable equivalence of the Gibbs criterion (largest pressure function p_i in the pure i -phase and equal pressures (12) in the mixed phase) and the

maximum entropy criteria (20) for an arbitrary equation of state $p = p(T)$ with a 1-st order phase transition. This equivalence is of fundamental importance for our consideration. The system is transformed into the mixed phase inside the energy density interval $[\varepsilon_W^c, \varepsilon_Q^c]$ as the entropy density of the mixed phase is the maximal one here.

The ratio of the total entropy of the created state to the number of nucleons participating in A+A collisions is given as

$$\frac{S}{2A} = \frac{V s}{2A} = \frac{m_N s}{\rho_0 \sqrt{s_{NN}}} \quad (21)$$

and it is independent on the number of participant nucleons. The entropy density s in Eq. (21) is given by our general expressions (20) with ε defined by Eq. (16). For small $\sqrt{s_{NN}}$ the energy density (16) corresponds to the pure W-state and one finds

$$\left(\frac{S}{2A}\right)_W = C g_W^{1/4} F, \quad (22)$$

where

$$C = \frac{2}{3} \left(\frac{\pi^2 m_N}{15 \rho_0}\right)^{1/4} \eta^{3/4}, \quad F = \frac{(\sqrt{s_{NN}} - 2m_N)^{3/4}}{(\sqrt{s_{NN}})^{1/4}}. \quad (23)$$

It gives a linear (proportional) increase of the entropy per baryon with F at small collision energy when pure W-state is formed. For high $\sqrt{s_{NN}}$ the pure Q-state is formed and Eq. (21) leads to

$$\begin{aligned} \left(\frac{S}{2A}\right)_Q &= C g_Q^{1/4} F \left(1 - \frac{2m_N B}{\eta \rho_0 (\sqrt{s_{NN}} - 2m_N) \sqrt{s_{NN}}}\right)^{3/4} \\ &\cong C g_Q^{1/4} F \left(1 - \frac{3m_N B}{2\eta \rho_0 F^4}\right). \end{aligned} \quad (24)$$

For large values of F the entropy per baryon in Q-state is also proportional to F . The slope of the linear function (24) is, however, larger than that in the W-state: $g_Q^{1/4}$ in Eq. (24) instead of $g_W^{1/4}$ in Eq. (22). Between ‘small’ ($F < F_1$) and ‘large’ ($F > F_2$) values of F there is a region of ‘intermediate’ collision energies ($F_1 < F < F_2$) where the mixed phase is formed according to the maximum entropy condition (20). In this region the energy dependence of the entropy per baryon is given by:

$$\left(\frac{S}{2A}\right)_{mix} = \frac{C_1}{\sqrt{s_{NN}}} + C_2 (\sqrt{s_{NN}} - m_N), \quad (25)$$

where

$$C_1 = \frac{m_N}{\rho_0} a, \quad C_2 = \eta b. \quad (26)$$

Eq. (25) gives approximately a F^2 increase of the entropy per baryon in the mixed phase region.

Let us now turn to strangeness and assume that g_W^s and g_Q^s are the numbers of internal degrees of freedom of (anti)strangeness carriers in W- and Q-state, respectively. The total

entropy of the considered state is given by a sum of entropies of strange and nonstrange degrees of freedom. Provided that all particles are massless the fraction of entropy carried by strange (and antistrange) particles is proportional to the number of strangeness degrees of freedom:

$$S_s = \frac{g^s}{g} S . \quad (27)$$

Eq. (27) is valid for both W- and Q-state. Note that all degeneracy factors are calculated according to the general relation (9). For massless particles of the i -th species the entropy is proportional to the particle number

$$S_i = 4N_i . \quad (28)$$

Thus the number of strange and antistrange particles can be expressed as

$$N_s + N_{\bar{s}} = \frac{S}{4} \frac{g^s}{g} , \quad (29)$$

and the strangeness per entropy is equal to

$$\frac{N_s + N_{\bar{s}}}{S} = \frac{1}{4} \frac{g^s}{g} . \quad (30)$$

Thus the strangeness per entropy for the ideal gas of massless particles is dependent only on the ratio of strange g^s to all g degrees of freedom. This ratio is expected to be equal to $g_Q^s/g_Q \cong 0.22$ in Q-state and $g_W^s/g_W \cong 0.5$ in W-state (see the next subsection). Therefore a phase transition from W- to Q-state should lead to a decrease of the strangeness to entropy ratio by a factor of about 2. This simple picture will be modified essentially because of the large in comparison to T value of the mass of strange degrees of freedom in W-state ($m_W^s \cong 500$ MeV). The left hand side of Eq.(30) becomes not a constant but a strongly increasing function of T . The right hand side of Eq.(30) gives then only its asymptotic value approached for $T \gg m_W^s$. The numerical calculations for the selected parameters of W- and Q-state are given below.

3.2 Numerical Calculations

The results of the calculations performed within the full version of the model as defined in Section 2 are presented below. We keep all non-strange degrees of freedom to be massless. The equations of the previous subsections are therefore valid for their thermodynamical functions. We use

$$g_Q^o = 2 \cdot 8 + \frac{7}{8} \cdot 2 \cdot 2 \cdot 3 \cdot 2 = 37 ; \quad g_W^o = 16 \quad (31)$$

for the non-strange degrees of freedom. The strange degrees of freedom are considered as massive ones. The equation (7) is used with

$$g_Q^s = 2 \cdot 2 \cdot 3 = 12 , \quad m_Q^s \cong 175 \text{ MeV} ; \quad g_W^s = 14 , \quad m_W^s \cong 500 \text{ MeV} . \quad (32)$$

Note that there is no factor $7/8$ in g_Q^s (32) as the equation (7) with Fermi momentum distribution and non-zero strange quark mass m_Q^s is now used. The contributions of

strange degrees of freedom into the entropy and energy densities are calculated with thermodynamical relations (6).

In order to demonstrate properties of the equation of state the energy and pressure divided by T^4 are plotted in Fig. 1 as a function of the temperature. The bag constant $B = 600 \text{ MeV/fm}^3$ was adjusted such that the critical temperature is $T_c = 200 \text{ MeV}$. This choice of T_c was suggested by the results of the analysis of hadron multiplicities in A+A collisions at SPS energies. They indicate that the hadron chemical freeze-out (or hadronization) occurs at a temperature 160–190 MeV [26, 27, 28, 23, 24].

As pointed out in the previous section a convenient variable to study collision energy dependence is the Fermi–Landau variable F . This variable is used for the further analysis. The relation of the F variable to the laboratory momentum p_{LAB} is shown in Fig. 2. The values of F for the top SPS and AGS energies are about $4 \text{ GeV}^{1/2}$ and $1.7 \text{ GeV}^{1/2}$, respectively.

The energy density can be calculated in a unique way on the base of points ‘3’ and ‘4’ from Section 2. The energy density (16) obtained in this way is plotted in Fig. 3 as a function of F ($\eta \cong 0.67$). The energy densities for the top SPS and AGS energies are about 12 GeV/fm^3 and 0.7 GeV/fm^3 , respectively.

The dependence of the early stage temperature T on F is shown in Fig. 4. Outside the transition region T increases in an approximately linear way. In the transition region T is constant $T = T_c = 200 \text{ MeV}$. The transition region begins at $F = F_1 = 2.23 \text{ GeV}^{1/2}$ ($p_{LAB} = 30 \text{ A}\cdot\text{GeV}$) and ends at $F = F_2 = 2.90 \text{ GeV}^{1/2}$ ($p_{LAB} = 64 \text{ A}\cdot\text{GeV}$).

The fraction of the volume occupied by the Q-state, ξ , increases rapidly in the transition region, as shown in Fig. 5.

The dependence of the entropy per baryon on F is shown in Fig. 6. Outside the transition region the entropy increases approximately proportionally to F , but the slope in the Q-state region is larger than the slope in the low energy region. The ratio between the value of entropy obtained in our model and the entropy calculated assuming absence of Q-state is shown in Fig. 7.

The strangeness to entropy ratio increases with the collision energy below the transition energy. This is due to the fact that the mass of the strange degrees of freedom is significantly higher than the system temperature. At $T = T_c$ the ratio is higher in W-state than in the Q-state, this causes the decrease of the ratio in the mixed phase to the level characteristic for Q-state. In the Q-state, due to the low mass of strange quark in comparison to the system temperature, only a weak dependence of the ratio on F is seen. The F dependence of strangeness/entropy ratio is shown in Fig. 8.

Within the model one can estimate the lower limit for $T_c = 170 \text{ MeV}$ ($B = 300 \text{ MeV/fm}^3$) which follows from the requirement that the transition energy should be above AGS top energy (15 A·GeV). In the case of $T_c = 170 \text{ MeV}$ the non-monotonic behaviour of strangeness production will be substituted by a rapid saturation. Remaining signatures of the phase transition will be unchanged.

4 Comaprison with Data

The comparison of the model with the experimental data on pion and strangeness production is presented below. The results are taken from the compilations [4, 5, 7] where the references to the original experimental publications can be found.

During the evolution of the system the equilibration between newly created matter and baryons take place. It is argued that this equilibration causes transfer of entropy from the produced matter to the baryonic sector. By analysis of the pion suppression effect at low collision energies one can roughly estimate that this transfer corresponds to the effective absorption of about 0.35 pion per participant nucleon [25]. We assume that there are no other processes which change the entropy content of the state produced in the early stage.

For the comparison with the model it is convenient to define the quantity:

$$\langle S_\pi \rangle = \langle \pi \rangle + \kappa \langle K + \bar{K} \rangle + \alpha \langle N_P \rangle, \quad (33)$$

where $\langle \pi \rangle$ is the measured total multiplicity of final state pions and $\langle K + \bar{K} \rangle$ is the multiplicity of kaons and antikaons. The factor $\kappa = 1.6$ is the approximate ratio between entropy per kaon to the entropy per pion at chemical freeze-out. The term $\alpha \langle N_P \rangle$ with $\alpha = 0.35$ is the above discussed correction for the entropy transfer to baryons. The quantity $\langle S_\pi \rangle$ can thus be interpreted as the early stage entropy measured in pion entropy units. The conversion factor between S and $\langle S_\pi \rangle$ is choosen to be 4 (\approx entropy per pion at chemical freeze-out).

The number of baryons which take part in the collision ($2A$ in the model calculations) is identified now with the experimentally measured number of participant nucleons, $\langle N_P \rangle$. The fraction of energy carried by the produced particles (η in Eq. 1) is taken to be 0.67 as measured by the NA35 Collaboration [30] for central S+S collisions at 200 A·GeV. Production of pions and kaons scales with the number of participant nucleons when central Pb+Pb and S+S collisions at SPS are compared [31]. This suggests that η can be assumed to be independent of the size of the colliding nuclei. Similar values of η are obtained when central A+A collisions at the AGS are analyzed [32] and the correction for the pion absorption is taken into account.

The comparison between the data on $\langle S_\pi \rangle / \langle N_P \rangle$ and the model is shown in Fig. 9. The description of the high energy (SPS) results obtained by the NA35 and NA49 Collaborations is essentially parameter free, as the properties of the early stage state, Quark Gluon Plasma, are well defined. The slope of the low energy dependence was adjuasted to the data, as the properties of W-state were assumed to be unknown. The change of the F depedence of the pion multiplicity was previously proposed as a signature of the transition region [6].

The comaprison between the model and the data on strangeness production is done under assumption that the strangeness content defined in the early stage is preserved till the hadronic freeze-out.

The total strangeness production is usually studied using the experimental ratio:

$$E_s = \frac{\langle \Lambda \rangle + \langle K + \bar{K} \rangle}{\langle \pi \rangle}, \quad (34)$$

where $\langle\Lambda\rangle$ is the mean multiplicity of Λ hyperons. Within the model E_s (34) is calculated as:

$$E_s = \frac{(N_s + N_{\bar{s}})/1.36}{(S - S_s)/4 - \alpha\langle N_P\rangle}, \quad (35)$$

where a factor 1.36 is the experimentally estimated ratio between total strangeness and strangeness carried by Λ hyperons and $K + \bar{K}$ mesons [33] and S_s is the fraction of the entropy carried by the strangeness carriers. The comparison between the calculations and the data is shown in Fig. 10. As in the case of the pion multiplicity, the description of the strangeness results at the SPS (NA35 and NA49 Collaborations) can be considered as being essentially parameter free⁴. The agreement in both cases is obtained assuming creation of globally equilibrated QGP in the early stage of nucleus–nucleus collisions. The description of the AGS data is obtained by fit of the internal number of strangeness degrees of freedom, which yields $g_W^s \approx 14$. The characteristic non-monotonic energy dependence of the E_s ratio was proposed in Ref. [5] as a signature of the phase transition and it is confirmed here by calculations in our model. Measurements of strangeness and pion production in the transition region are obviously needed.

The entropy and strangeness production in central A+A collisions considered here satisfies well the conditions needed for thermodynamical treatment. Therefore one expects that both the entropy per participant, $\langle S_\pi \rangle / \langle N_P \rangle$, and strangeness per entropy, E_s , are independent on the number of participants for large enough values of $\langle N_P \rangle$. In order to check this in an explicit way we show $\langle S_\pi \rangle / \langle N_P \rangle$ (Fig. 11) and E_s (Fig. 12) as a function of $\langle N_P \rangle$ at SPS energy for central S+S and Pb+Pb collisions.

⁴ The E_s value resulting from a QGP can be estimated in a simple way. Assuming that $m_s = 0$, and neglecting small ($< 5\%$) effect of pion absorption at SPS, one gets from (30) and (35) $E_s \approx (g_Q^s/1.36)/g_Q^{ns} \approx 0.21$, where $g_Q^s = (7/8) \cdot 12$ is the effective number of degrees of freedom of s and \bar{s} quarks and $g_Q^{ns} = 16 + (7/8) \cdot 24$ is the corresponding number for u, \bar{u}, d, \bar{d} quarks and gluons. Here we use also approximation that the mean entropy per pion at chemical freeze-out is equal to the mean entropy per q, \bar{q} and g in a QGP.

5 Discussion

Relations between our approach and two widely discussed aspects of nucleus–nucleus collisions strangeness and J/Ψ production are presented. Finally we comment on the event–by–event fluctuations.

5.1 Strangeness Production

The enhanced production of strangeness was considered by many authors as a potential signal of QGP formation [9, 10, 11]. The line of arguments is the following. One estimates that the strangeness equilibration time in QGP is comparable to the duration of the collision process (< 10 fm/c) and about 10 times shorter than the corresponding equilibration time in hadronic matter. It is further assumed that in the early stage strangeness density is much below the equilibrium density e.g. it is given by the strangeness obtained from the superposition of nucleon–nucleon interactions. Thus it follows that during the expansion of the matter the strangeness content increases rapidly and approaches its equilibrium value provided the matter is in the QGP state. In the case of hadronic matter the modification of the initial strangeness content is less significant due to the long equilibration time. This leads to the expectation that strangeness production should rapidly increase when the energy transition region is crossed from below.

In the model presented in this paper the role of strangeness is different. The reason for that is different assumption concerning the early stage properties. We assume that due to the statistical nature of the creation process the strangeness in the early stage is already at equilibrium and therefore possible secondary processes do not modify it. As at $T = T_c$ the strangeness density is similar or even lower (depending on the T_c value) in the QGP than in the confined matter, saturation or suppression of strangeness production is expected to occur when crossing the transition energy range from below.

In our model the low level of strangeness production in N+N interactions as compared to the strangeness yield in central A+A collisions, called strangeness enhancement, can be understood as due to the effect of strict strangeness conservation (canonical suppression factor) imposed on the degrees of freedom in the confined matter in the early stage.

5.2 J/Ψ Production

Suppression of J/Ψ production was proposed as a signal of creation of the QGP in nuclear collisions [34]. The details of the models used to describe the process changed with time, but the main line of arguments, important here, is the same since the first proposal (for a recent review see [16]). The interpretation of J/Ψ results is done within hard production QCD model. It is assumed that the creation of J/Ψ follows the dependence given by the production of Drell–Yan pairs, i.e. the inclusive cross section in A+A collisions increases with A as A^2 . Deviations from this dependence are interpreted as due to interaction of the J/Ψ (or ‘pre- J/Ψ ’ state) with the surrounding matter. Suppression of J/Ψ observed in p+A and O(S)+A collisions at SPS is interpreted as due to the interactions with participant nucleons and produced particles. The rapid increase of the suppression observed

only for central Pb+Pb collisions is attributed [35, 36, 17] to the formation of the QGP which leads to large additional absorbtion of the created J/Ψ .

This interpretation is in contradiction to the conclusions based on the analysis of pion and strangeness results within the statistical model. No anomalous change in this observables is seen between central S+S and cental Pb+Pb collisions (see Figs. 11 and 12) when studing these observables. It is therefore essential to understand whether this contradiction can be removed when the same approach is used to interpret the whole set of data.

It is natural to extend our statistical model for charm production assuming that like entropy and strangeness, charm in the early stage is produced according to the phase space. We take the mass of the charm quark to be $m_Q^c \cong 1.5$ GeV and calculate the mean number of c and \bar{c} quarks for central Pb+Pb collisions at 158 A·GeV. The early stage volume (2) for the experimental number of nucleon participants $\langle N_P \rangle$ in central Pb+Pb collisions is approximately $V \cong 200 \text{ fm}^3$. For the number density of c plus \bar{c} we find ($g_Q^c = 2 \cdot 2 \cdot 3 = 12$):

$$\rho_{c\bar{c}} = \frac{g_Q^c}{2\pi^2} \int_0^\infty k^2 dk \frac{1}{\exp\left(\frac{\sqrt{k^2 + (m_Q^c)^2}}{T}\right) + 1} \cong g_Q^c \left(\frac{m_Q^c T}{2\pi}\right)^{3/2} \exp\left(-\frac{m_Q^c}{T}\right). \quad (36)$$

With the model temperature $T \cong 264$ MeV (see Fig. 4) equation (36) gives the total average number of charm quarks and antiquarks

$$N_{c\bar{c}} = \rho_{c\bar{c}} V \cong 17. \quad (37)$$

The equilibrium number (37) of c and \bar{c} quarks which are hadronize mainly into D-mesons exceeds substantially the recent estimates given in Ref. [37]. The equilibrium number seems to be also higher than the upper limit estimated from the $\mu^+\mu^-$ invariant mass spectrum measured in central Pb+Pb collisions [38]. This estimate, however, strongly depend on the assumed shape of the dimuon spectrum.

We consider also the possible influence of a strict charm conservation. In Fig. 13 we show the predicted dependence of the charm/entropy ratio on the number of participant nucleons ($2A$) including a correction for strict charm conservation calculated as in Ref. [39]. It is observed that even down to low values of $2A = 40$ the correction is small and therefore the charm/entropy ratio is approximately independent of the volume of the system, similar to the strangeness/entropy ratio.

Analysis of the hadron yields within a statistical hadronization model [23, 24] shows that the hadronization is a local statistical process. Thus one expects that also the mean J/Ψ multiplicity per entropy (pion multiplicity) should be volume independent. This prediction of our model can be now checked against experimental data. However as the data on J/Ψ multiplicity are not published, we have to perform ourselves a conversion of the available data. We use the the E_T dependence of the ratio measured by the NA50 Collaboration [40]:

$$R(J/\Psi) = \frac{B_{\mu\mu}\sigma(J/\Psi)}{\sigma(DY)}, \quad (38)$$

where $\sigma(J/\Psi)$ and $\sigma(DY)$ are inclusive cross sections for production of J/Ψ and Drell–Yan pairs and $B_{\mu\mu}$ is the branching ratio of J/Ψ decay into a $\mu^+\mu^-$ pair. As at SPS energies pion production dominates particle production, the measured transverse energy is basically determined by the pion transverse energy. The mean transverse momentum of pions is independent of the centrality [41] and therefore E_T can be considered to be proportional to the pion multiplicity or the number of participant nucleons. The multiplicity of Drell–Yan pairs increases with the centrality as $\langle N_P \rangle^{4/3}$ or equivalently as $E_T^{4/3}$. Thus the mean J/Ψ multiplicity is expected to increase in our estimation as:

$$\langle J/\Psi \rangle \sim R(J/\Psi) E_T^{4/3} \quad (39)$$

and consequently the J/Ψ multiplicity per pion should be proportional to

$$\frac{\langle J/\Psi \rangle}{E_T} \sim R(J/\Psi) E_T^{1/3}. \quad (40)$$

The values of $R(J/\Psi) E_T^{1/3}$ are plotted as a function of E_T for Pb+Pb collisions at 158 A·GeV in Fig. 14. The ratio $R(J/\Psi) E_T^{1/3} (\sim \langle J/\Psi \rangle / \langle \pi \rangle)$ is independent of E_T in the whole range of E_T . Thus we conclude that the experimental dependence of J/Ψ production on E_T in Pb+Pb collisions is in the agreement with the expectation of our model. It just reflects the statistical character of charm production and the following hadronization process.

As pointed out in Ref. [24] the particle abundances resulting from the hadronization process can be modified by the inelastic interactions in the freeze-out hadronic matter. It is however argued [16] that the J/Ψ hadronic cross sections are small, thus no significant reduction of the J/Ψ yield is expected by hadronic processes. This argumentation is however not valid for Ψ' production for which hadronic cross sections are estimated to be 10 times larger than for J/Ψ and therefore a significant suppression of Ψ' due to hadronic interactions can be expected [16]. This is usually considered as the reason why the ratio $\sigma(\Psi')/\sigma(J/\Psi)$ decreases with E_T [16].

We summarize that the effect of the anomalous J/Ψ suppression in central Pb+Pb collisions is a result of the interpretation of the data within the model of hard QCD production of J/Ψ with following suppression. The same data analyzed within the statistical approach show no anomalous behaviour and lead to a consistent interpretation of the results on pion, strangeness and charm production.

5.3 Event–by–Event Fluctuations

It was recently measured by the NA49 Collaboration [42] that the event–by–event transverse momentum fluctuations in central Pb+Pb collisions at 158 A·GeV are much smaller than the fluctuations measured in the p+p interactions and expected in non–equilibrium models of nuclear collisions [43, 44]. A decrease of the global fluctuations with the increasing volume of the system and/or increasing number of internal degrees of freedom is a generic feature of the statistical models [45]. Therefore in our approach one expects a decrease of global fluctuations when going from p+p interactions to central Pb+Pb collisions. The same arguments lead to the conclusion that the flavour fluctuations should be

also reduced in central A+A collisions in comparison to p+p interactions. The method to analyze these fluctuations was recently formulated [46].

Finally we expect an increase of the fluctuations in the transition region. This is because of the additional possibility of changing the relative content of W⁻ and Q-state in the early stage. An important observable should be the strangeness to entropy ratio as it is significantly different in W⁻ and Q-state at $T = T_C$.

6 Summary and Conclusions

In this paper we continue the development of a statistical model of the early stage in high energy nucleus–nucleus collisions. We attempt to understand the possible meaning of the equilibration of the *created state*. We attribute the success of the statistical description of the early stage to the statistical nature of the QCD production process in A+A collisions rather than to the results of multiple secondary processes following the primary creation.

We show that the assumption that the state created in the early stage is in the form of the Quark Gluon Plasma gives an essentially parameter free description of the data on pion and strangeness production in central A+A collisions at SPS.

It is argued that the early stage degrees of freedom in the confined matter can not be modeled by hadrons and hadronic resonances. An effective statistical description of the confined state (W–state) is introduced and the parameters characterizing degrees of freedom are extracted from the comparison with the data.

The transition between W–state and QGP when increasing collision energy is discussed. It is proven that the condition of maximum entropy is equivalent to the Gibbs construction of the first order phase transition between W–state and QGP.

The transition region is localized to be between 30 A·GeV and 65 A·GeV for the set of parameters used in the paper. It is shown that the transition should be associated with a rapid increase of pion multiplicity and a non–monotonic energy dependence of the strangeness to pion ratio. It is also argued that an increase of the event–by–event fluctuations can be expected in the transition region. Note that anomalies in the space–time pattern of the matter expansion are also expected due to softening of the equation of state in the mixed phase [29]. This can be detected by the analysis of single particle spectra and two particle correlations [47].

Finally we remind that the anomalous J/Ψ suppression in central Pb+Pb collisions at SPS is a result of the data interpretation within a model assuming that the charm production is a hard QCD process. We show that the same results are also consistent with the hypothesis that the J/Ψ multiplicity per pion is independent of the centrality of Pb+Pb collisions, similar to the behaviour of the strangeness/pion ratio. This behaviour can be reproduced in our approach when the charm production is treated in the same statistical way as the production of strangeness. This allows for a consistent interpretation of the results on pion, strangeness and J/Ψ production in A+A collisions at SPS. Data on total charm production are obviously needed to check our assumption of statistical charm production.

We conclude that a broad set of experimental data is in agreement with the hypothesis that QGP is created in central A+A (S+S and Pb+Pb) collisions at the SPS. A study of the energy dependence of several basic observables (pion and strangeness multiplicities, expansion pattern and event–by–event fluctuations) should be able to uniquely prove the existence of the QCD phase transition to the Quark Gluon Plasma.

Appendix A

The properties of W-state were obtained by an ‘educated guess’ procedure. It is however still interesting to note that the degrees of freedom in W-state can be identified with colourless $q\bar{q}$ pairs. Assuming that the light quarks (u, d) are almost massless we obtain 4 non-strange flavour-antiflavour combinations: $u\bar{u}, d\bar{d}, d\bar{u}$ and $u\bar{d}$. Each pair can be in 4 spin states, which gives 16 massless non-strange internal degrees of freedom. Similar counting gives 16 different pairs containing s or \bar{s} quark. There are in addition 4 $s\bar{s}$ pairs which however can be considered strongly suppressed due to the large mass of strange quarks. Thus the numbers of non-strange and strange degrees of freedom obtained for the colourless $q\bar{q}$ pairs approximately coincide with the corresponding numbers extracted from the data for the W-state ($g_W^{ns} \approx 16$ and $g_W^s \approx 14$).

The reduction of the effective number of degrees of freedom from colored q, \bar{q} and g to colour neutral $q\bar{q}$ pairs may be understood as a result of the requirement of local colour neutrality imposed on the creation process at low energy density and/or for small systems.

We note also that the colourless $q\bar{q}$ pairs are identified as initial degrees of freedom in the $e^+ + e^-$ annihilation process by the well known analysis of the ratio $\sigma(e^+ + e^- \rightarrow \text{hadrons})/\sigma(e^+ + e^- \rightarrow \mu^+ + \mu^-)$ [22].

Appendix B

We present here a general proof of the equivalence between Gibbs construction of the 1-st order phase transition and the basic condition that the equilibrium state is equal to the maximum entropy state. The proof is valid when all conserved charges are equal to zero as considered in the paper. In this case the pressure function, $p = p(T)$, defines completely the system thermodynamics providing that the system volume V goes to infinity (thermodynamical limit). The temperature T remains the only independent thermodynamical variable. The energy density, $\varepsilon(T)$, and entropy density, $s(T)$, are calculated as

$$\varepsilon(T) = T \frac{dp}{dT} - p, \quad s(T) = \frac{dp}{dT}. \quad (41)$$

A discontinuity of first derivative, dp/dT , at $T = T_c$ corresponds, by definition, to a 1-st order phase transition at temperature $T = T_c$. In physical terms one describes the system at $T < T_c$ by function $p = p_1(T)$ (low-temperature phase) and by $p = p_2(T)$ at $T > T_c$ (high-temperature phase). At $T = T_c$ pressures of the two phases are equal

$$p_1(T_c) = p_2(T_c) \equiv p_c, \quad (42)$$

and their first derivatives satisfy inequalities

$$\left(\frac{dp_2}{dT} \right)_{T=T_c} > \left(\frac{dp_1}{dT} \right)_{T=T_c}. \quad (43)$$

The energy density discontinuity (latent heat) as well as the entropy density discontinuity take place at $T = T_c$:

$$\Delta\varepsilon = \varepsilon_2(T_c) - \varepsilon_1(T_c) = T_c [s_2(T_c) - s_1(T_c)] > 0. \quad (44)$$

At $T = T_c$ the system is in the mixed phase with

$$\varepsilon_{mix} = (1 - \xi)\varepsilon_1(T_c) + \xi\varepsilon_2(T_c), \quad s_{mix} = (1 - \xi)s_1(T_c) + \xi s_2(T_c), \quad (45)$$

where $1 - \xi$ and ξ are relative volumes occupied by phases ‘1’ and ‘2’, respectively. The above construction is known as the Gibbs criteria for a 1-st order phase transition: at a given temperature T the system occupies a pure phase which pressure is larger and the mixed phase is formed if both pressures are equal. One considers phases ‘1’ at $T > T_c$ and ‘2’ at $T < T_c$ as metastable states (superheated and supercooled, respectively). Such a consideration is physically important in the kinetic picture of a phase transition and for the studies of statistical fluctuations. We prove now the equivalence of the Gibbs criteria to the maximum entropy condition of the mixed phase. It claims that at any energy density ε from the interval $[\varepsilon_1(T_c), \varepsilon_2(T_c)]$ the entropy density of the mixed phase is maximal one:

$$s_{mix}(\varepsilon) > s_i(\varepsilon), \quad i = 1, 2, \quad \varepsilon \in [\varepsilon_1(T_c), \varepsilon_2(T_c)]. \quad (46)$$

The following equations for the entropy densities of the pure and mixed phase can be easily obtained from Eq. (41):

$$s_i = \frac{\varepsilon + p_i(T)}{T}, \quad i = 1, 2; \quad s_{mix} = \frac{\varepsilon + p_c}{T_c}. \quad (47)$$

These values of s_i and s_{mix} should be compared at the same ε from the interval $[\varepsilon_1(T_c), \varepsilon_2(T_c)]$. It requires $T > T_c$ for $i=1$ and $T < T_c$ for $i=2$ in Eq. (47). In order to compare s_i and s_{mix} we substitute ε in Eq. (47) by $Tdp_i/dT - p_i(T)$ according to Eq. (41). The inequalities (46) are then transformed into

$$\frac{dp_1}{dT} > \frac{p_1(T) - p_c}{T - T_c}, \quad T > T_c, \quad (48)$$

$$\frac{dp_2}{dT} < \frac{p_c - p_2(T)}{T_c - T}, \quad T < T_c. \quad (49)$$

Simple geometrical meaning of these inequalities is quite clear: they are satisfied for any convex (from below) function $p_i(T)$. Any physical pressure function $p(T)$ should have positive second derivative, $d^2p/dT^2 > 0$, and, therefore, is indeed a convex function. To prove this last statement we use the relation

$$\frac{d^2p}{dT^2} = \frac{1}{T} \frac{d\varepsilon}{dT}, \quad (50)$$

which follows from Eq. (41). Positive sign of $d\varepsilon/dT$ is a consequence of the definition of energy in statistical mechanics:

$$\varepsilon = \frac{\langle E \rangle}{V} = \frac{1}{V} \frac{\sum_n E_n \exp(-E_n/T)}{\sum_n \exp(-E_n/T)}. \quad (51)$$

From Eq. (51) one finds

$$\frac{d\varepsilon}{dT} = \frac{1}{V} \frac{d\langle E \rangle}{dT} = \frac{\langle E^2 \rangle - \langle E \rangle^2}{VT^2} = \frac{\langle (E - \langle E \rangle)^2 \rangle}{VT^2} > 0. \quad (52)$$

Acknowledgements

The results obtained by the NA35 and NA49 Collaborations play a major role in the interpretation of the whole set of data. We would like specially thank P. Seyboth and R. Stock spokesmen of these experiments. We thank K.A. Bugaev, D. Ferenc, L. Frankfurt, U. Heinz, C. Lourenco, St. Mrówczyński and B. Svetitsky for critical and vivid discussions and comments to the manuscript. M.I.G. is also grateful to the BMFT, DFG and GSI for the financial support.

References

- [1] Proceedings of Thirteen International Conference on Ultra Relativistic Nucleus–Nucleus Collisions, December 1–5, 1997, Tsukuba, Japan, to be published in Nucl. Phys. **A**.
- [2] E. Fermi, Prog. Theor. Phys. **5** (1950) 570.
- [3] L. D. Landau, Izv. Akad. Nauk SSSR, Ser. Fiz. **17** (1953) 51.
- [4] M. Gaździcki and D. Röhrich, Z. Phys. **C65** (1995) 215.
- [5] M. Gaździcki and D. Röhrich, Z. Phys. **C71** (1996) 55.
- [6] M. Gaździcki, Z. Phys. **C66** (1995) 659.
- [7] M. Gaździcki, J. Phys. **G23** (1997) 1881 (nucl-th/9706036).
- [8] L. Van Hove, Phys. Lett. **B118** (1982) 138.
- [9] P. Koch, B. Müller and J. Rafelski, Phys. Rep. **142** (1986) 321.
- [10] J. Kapusta and A. Mekjan, Phys. Rev. **D33** (1986) 1304.
- [11] T. Matsui, B. Svetitsky and L.D. McLerran, Phys. Rev. **D34** (1986) 783 and Phys. Rev. **D34** (1986) 2074.
- [12] F. Karsch, Nucl. Phys. **A590** (1995) 367c,
E. Laermann, Nucl. Phys. **A610** (1996) 1c.
- [13] M. Gaździcki et al. (NA35 and NA49 Collab.), Nucl. Phys. **A590** (1995) 197c,
M. Gaździcki and U. Heinz, Phys. Rev. **C54** (1996) 1496.
- [14] S. Jeon and J. Kapusta, Phys. Rev. **C56** (1997) 468.
- [15] J. Bächler et al. (NA49 Collaboration), *Status and Future Programme of the NA49 Collaboration*, CERN/SPSC 98–4 (1998).
- [16] C. Gerschel and J. Hüfner, *Charmonium suppression in heavy-ion collisions*, e-print hep-ph/9802245.
- [17] H. Satz, *Colour Deconfinement and J/Ψ Suppression in High Energy Nuclear Collisions* e-print hep-ph/9711289.
- [18] S. Pokorski and L. Van Hove, Acta Phys. Pol. **B5** (1974) 229,
L. Van Hove and S. Pokorski, Nucl. Phys. **B86** (1975) 243.
- [19] H. Leutwyler, Phys. Lett. **B378** (1996) 313.
- [20] E. V. Shuryak, Phys. Rep. **61**, (1980) 71,
J. Cleymans, R. V. Gavai and E. Suhonen, Phys. Rep. **130**, (1986) 217.

- [21] G.D. Yen, M.I. Gorenstein, W. Greiner and S.N. Yang, Phys. Rev. **C56** (1997) 2210.
- [22] D. H. Perkins, *Introduction to High Energy Physics*, Addison–Wesley Publishing Company (1982).
- [23] F. Becattini, Z. Phys. **C69** (1996) 485,
F. Becattini and U. Heinz, Z. Phys. **C76** (1997) 269 (hep-ph/9702274).
- [24] F. Becattini, M. Gaździcki and J. Sollfrank, *On Chemical Equilibrium in Nuclear Collisions*, e-print hep-ph/9710529, to be published in Eur. Phys. J. **C**.
- [25] M. Gaździcki, M. I. Gorenstein and St. Mrówczyński, *On Pion Suppression in Nuclear Collisions*, e-print nucl-th/9701013, to be published in Eur. Phys. J. **C**.
- [26] J. Cleymans and H. Satz, Z. Phys. **C57**, (1993) 135; J. Cleymans, K. Redlich, H. Satz and E. Suhonen, Z. Phys. **C58** (1993) 347 and Nucl. Phys. **A566** (1994) 391c.
- [27] P. Braun-Munzinger, J. Stachel, J. P. Wessels, and N. Xu, Phys. Lett. B **B365** (1995) 1; J. Stachel, Nucl. Phys. **A610** (1996) 509c.
- [28] R.A. Ritchie, M.I. Gorenstein and H.G. Miller, Z. Phys. **C75** (1997) 535.
- [29] C. M. Huang and E. Shuryak, Phys. Rev. Lett. **75** (1995) 4003.
- [30] J. Bächler et al., (NA35 Collab.), Phys. Rev. Lett. **72** (1994) 1419.
- [31] S. V. Afanasjev et al., (NA49 Collab.), Nucl. Phys. **A610** (1996) 188c.
- [32] H. Ströbele, Nucl. Phys. **A610** (1996) 102c, note that the values of inelasticity for S+S and Pb+Pb collisions at SPS are plotted incorrectly [30].
- [33] H. Białkowska, M. Gaździcki, W. Retyk and E. Skrzypczak, Z. Phys. **C55** (1992) 491.
- [34] T. Matsui and H. Satz, Phys. Lett. **178B** (1986) 416.
- [35] J.–P. Blaizot, J.–Y. Ollitrault, Phys. Rev. Lett. **77** (1997) 1703.
- [36] D. Kharzeev, M. Nardi and H. Satz, *Anomalous J/Ψ Suppression and the Nature of Deconfinement*, e-print hep-ph/9707308.
- [37] P. Braun–Munzinger et al., Eur. Phys. J. **C1** (1998) 123.
- [38] M. C. Abreu et al. (NA50 Collab.), Nucl. Phys. **A610** (1996) 331c.
- [39] J. Rafelski, M. Danos, Phys. Lett. **B97** (1980) 279.
- [40] L. Ramello et al. (NA50 Collab.), Proceedings of Thirteen International Conference on Ultra Relativistic Nucleus–Nucleus Collisions, December 1–5, 1997, Tsukuba, Japan, to be published in Nucl. Phys. **A**.

- [41] T. Alber et al. (NA35 Collab.), *Charged Particle Production in Proton, Deuteron, Oxygen and Sulphur Nucleus Collisions at 200 GeV per Nucleon*, hep-ex/9711001, to be published Eur. Phys. J. **C**.
- [42] G. Roland et al. (NA49 Collab.), Proceedings of Thirteen International Conference on Ultra Relativistic Nucleus–Nucleus Collisions, December 1–5, 1997, Tsukuba, Japan, to be published in Nucl. Phys. **A**.
- [43] M. Gaździcki and St. Mrówczyński, Z. Phys. **C54** (1992) 127.
- [44] M. Gaździcki, A. Leonidov and G. Roland, *On Event-by-Event Fluctuations in Nuclear Collisions*, e-print hep-ph/9711422, submitted to Eur. Phys. J. **C**.
- [45] L. Stodolsky, Phys. Rev. Lett. **75** (1995) 1044.
- [46] M. Gaździcki, *A Method to Study Chemical Equilibration in Nucleus–Nucleus Collisions*, nucl-th/9712050.
- [47] K. S. Lee, U. Heinz and E. Schnedermann, Z. Phys. **C48** (1990) 525,
U. Wiedemann, B. Tomasik and U. Heinz, *Reconstructing the Source in Heavy Ion Collisions from Particle Interferometry*, e-print nucl-th/9801017.

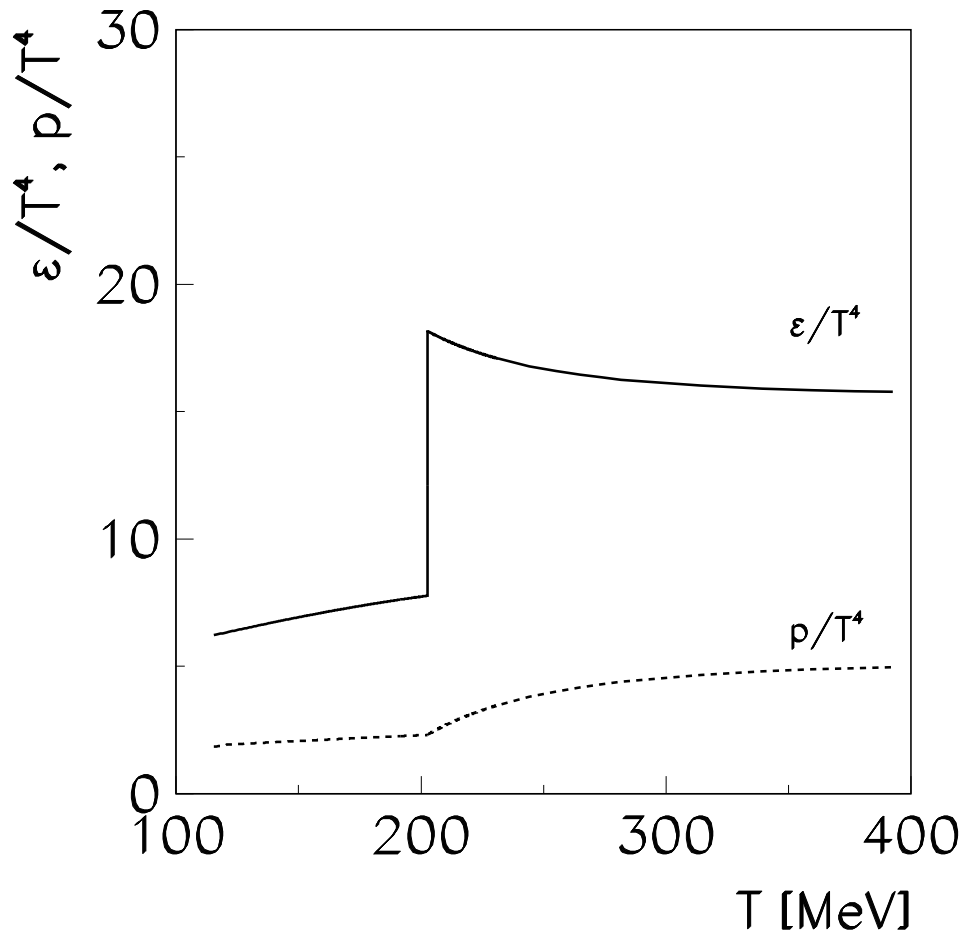


Figure 1: Energy density and pressure divided by T^4 as a function of temperature T .

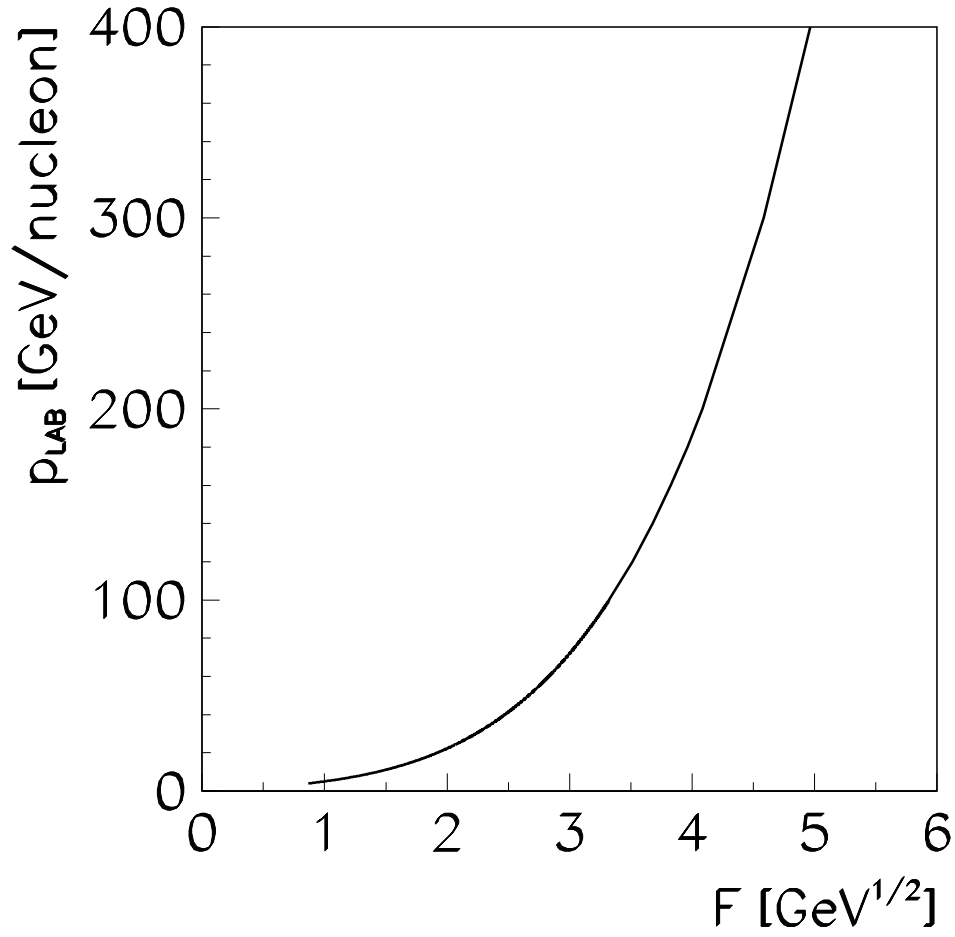


Figure 2: Relation between laboratory momentum per nucleon and the Fermi–Landau energy variable F . The values of F for $p_{LAB} = 5, 10, 15, 40, 80, 160$ and 200 A·GeV are 0.99, 1.43, 1.71, 2.47, 3.10, 3.82 and 4.08 GeV^{1/2}, respectively.

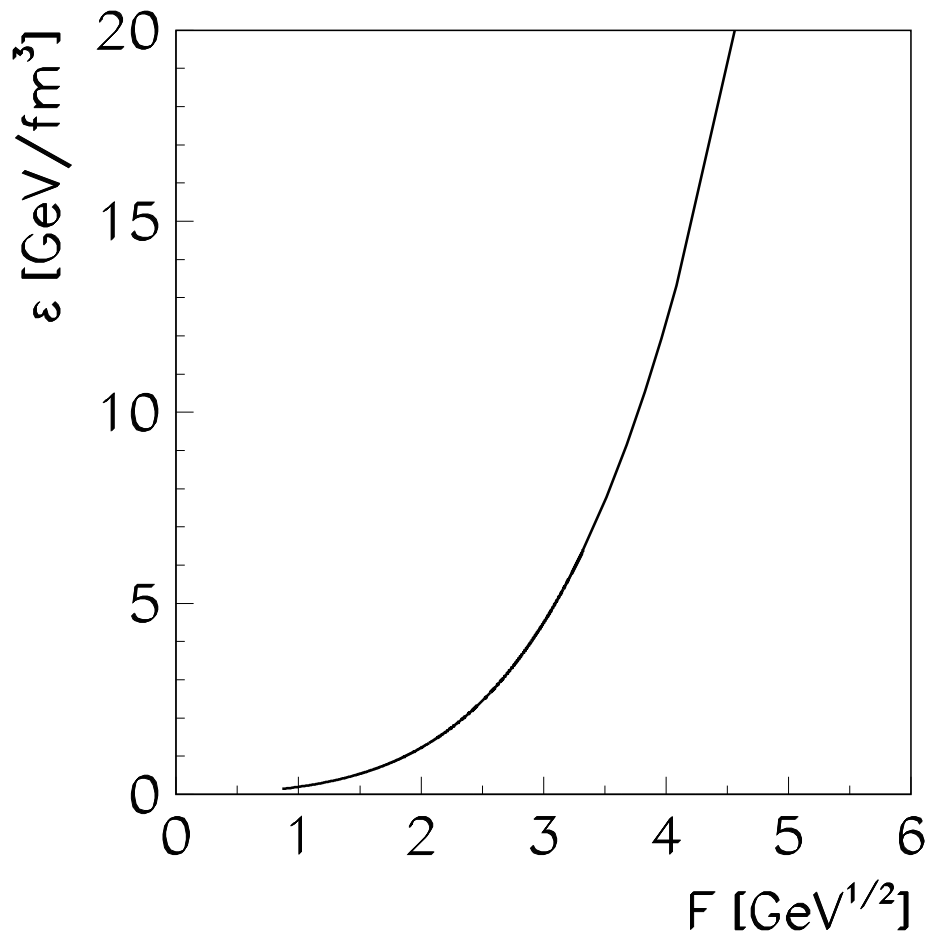


Figure 3: The early stage energy density as a function of F . The values of ϵ for $F = 0.99, 1.43, 1.71, 2.47, 3.10, 3.82$ and $4.08 \text{ GeV}^{1/2}$ are $0.20, 0.47, 0.77, 1.71, 2.36, 5.03, 10.53$, and 13.32 GeV/fm^3 , respectively.

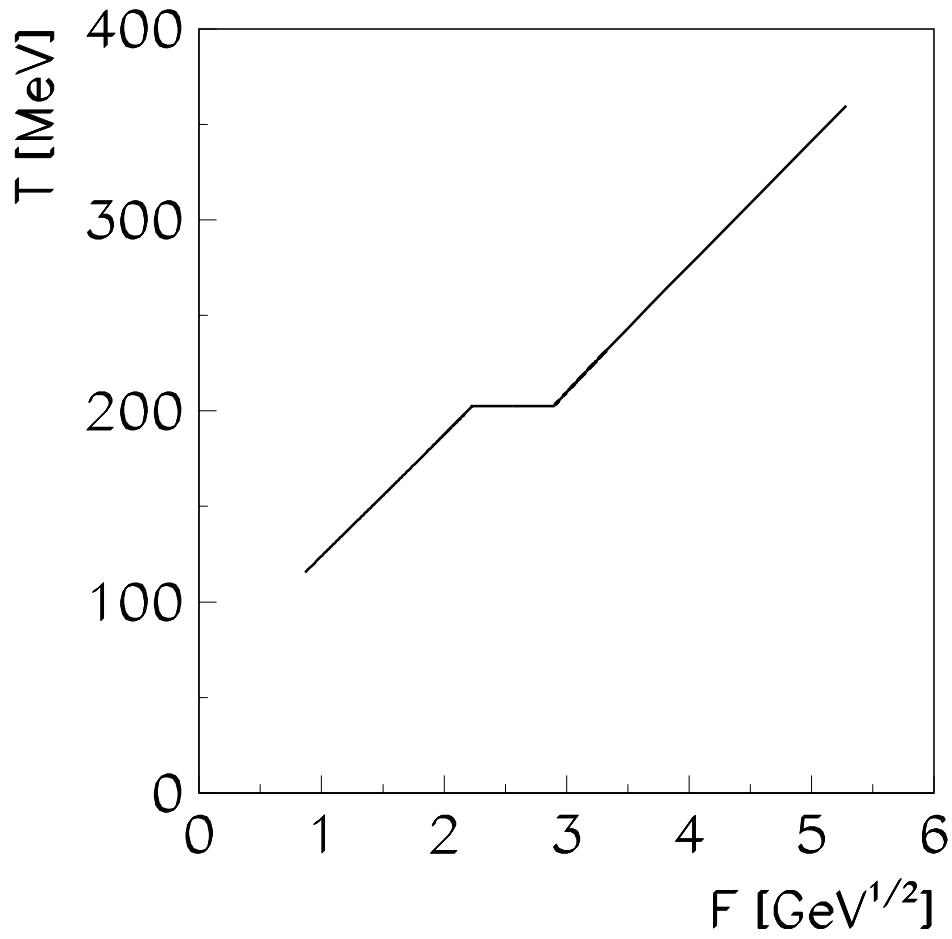


Figure 4: The early stage temperature as a function of F . The values of T for $F = 0.99, 1.43, 1.71, 2.47, 3.10, 3.82$ and 4.08 GeV $^{1/2}$ are 123, 151, 169, 218, 217, 264 and 281 MeV, respectively.

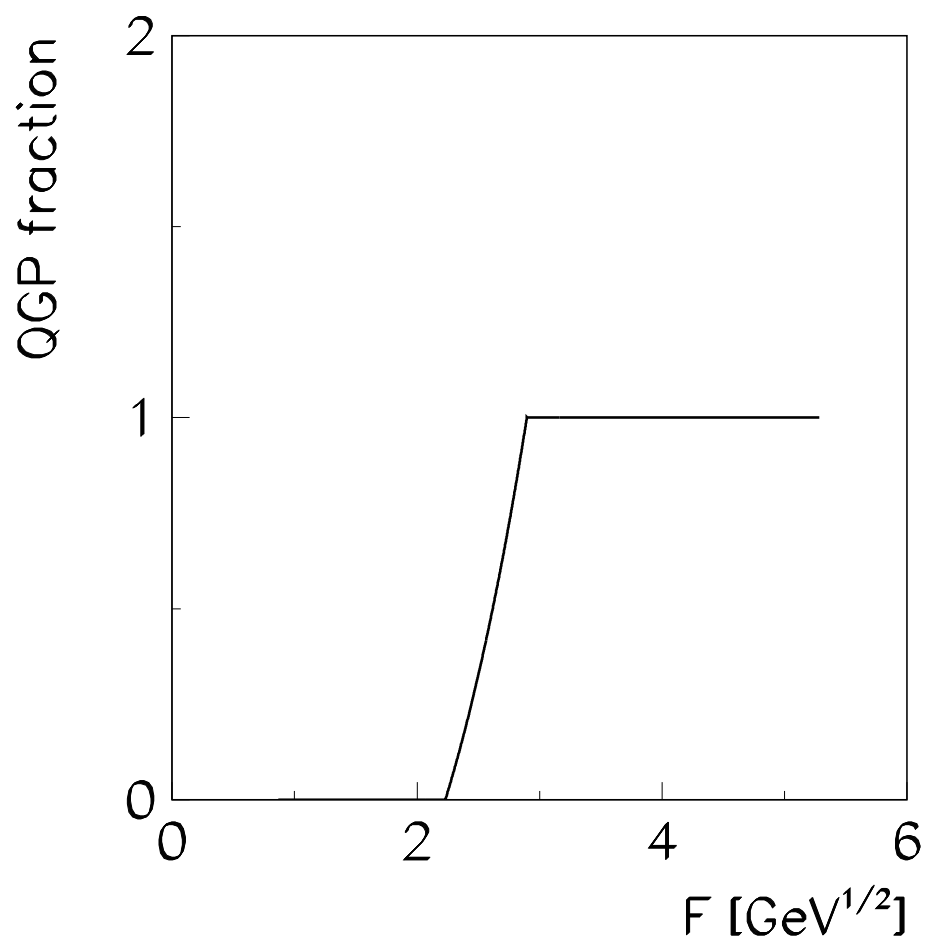


Figure 5: The fraction of volume occupied by a QGP as a function of F .

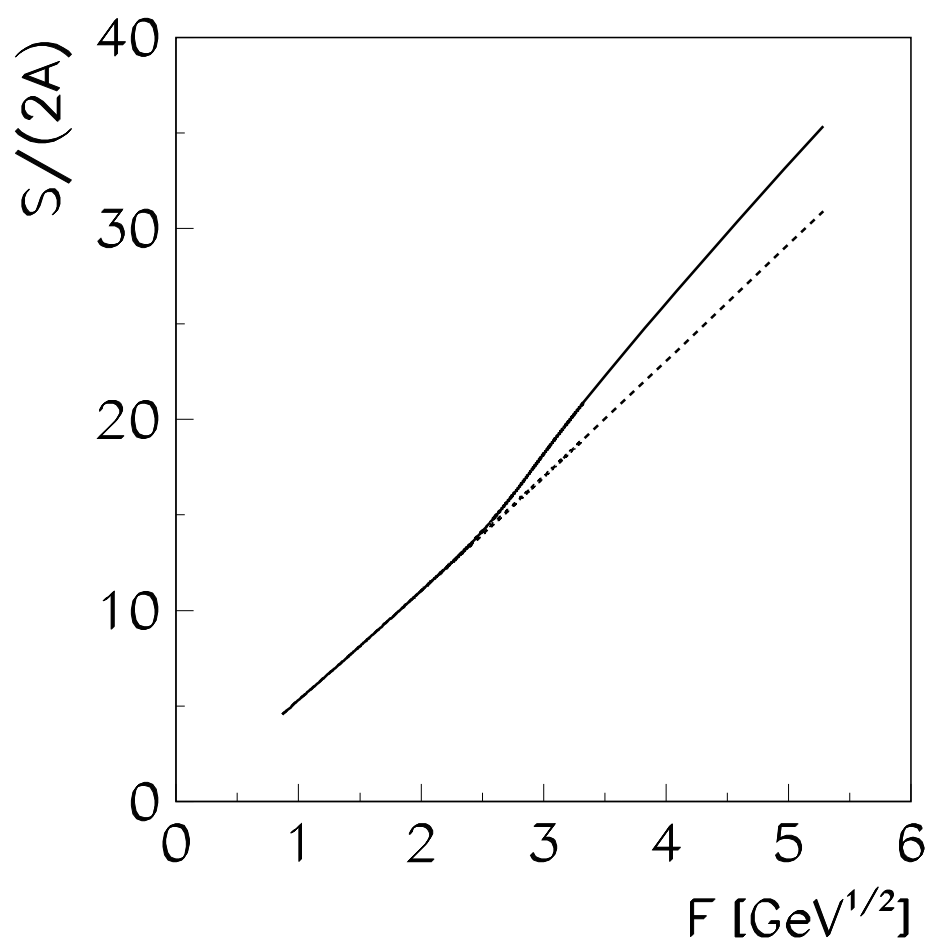


Figure 6: The entropy per baryon as a function of F (solid line). Dashed line indicates the dependence obtained assuming that there is no transition to QGP.

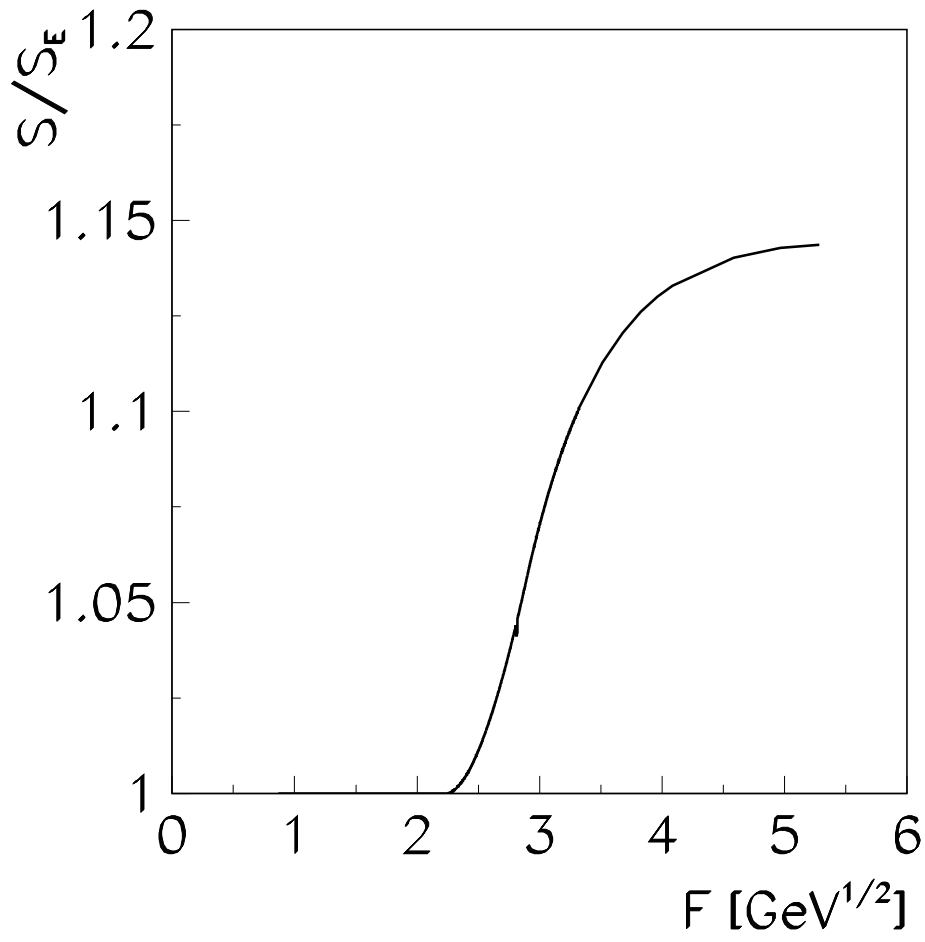


Figure 7: The ratio between the entropy calculated within our model and the entropy obtained assuming absence of phase transition to QGP.

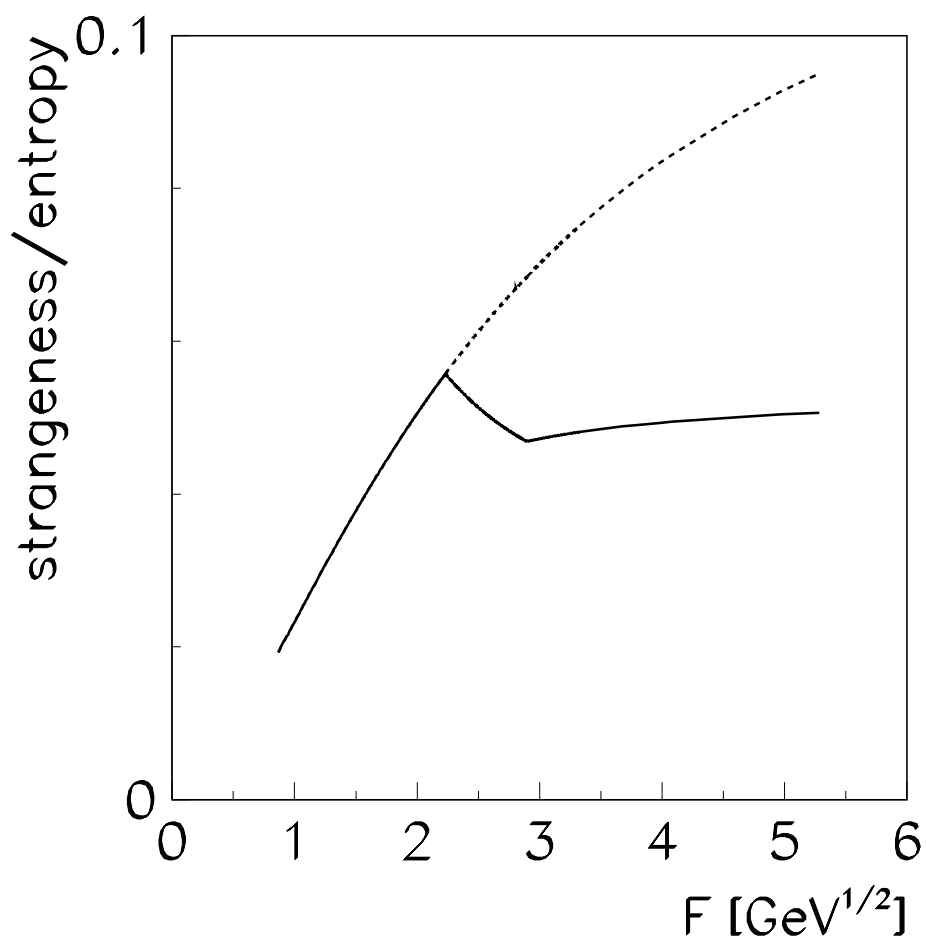


Figure 8: The ratio of the total number of s and \bar{s} quarks and antiquarks to the entropy.

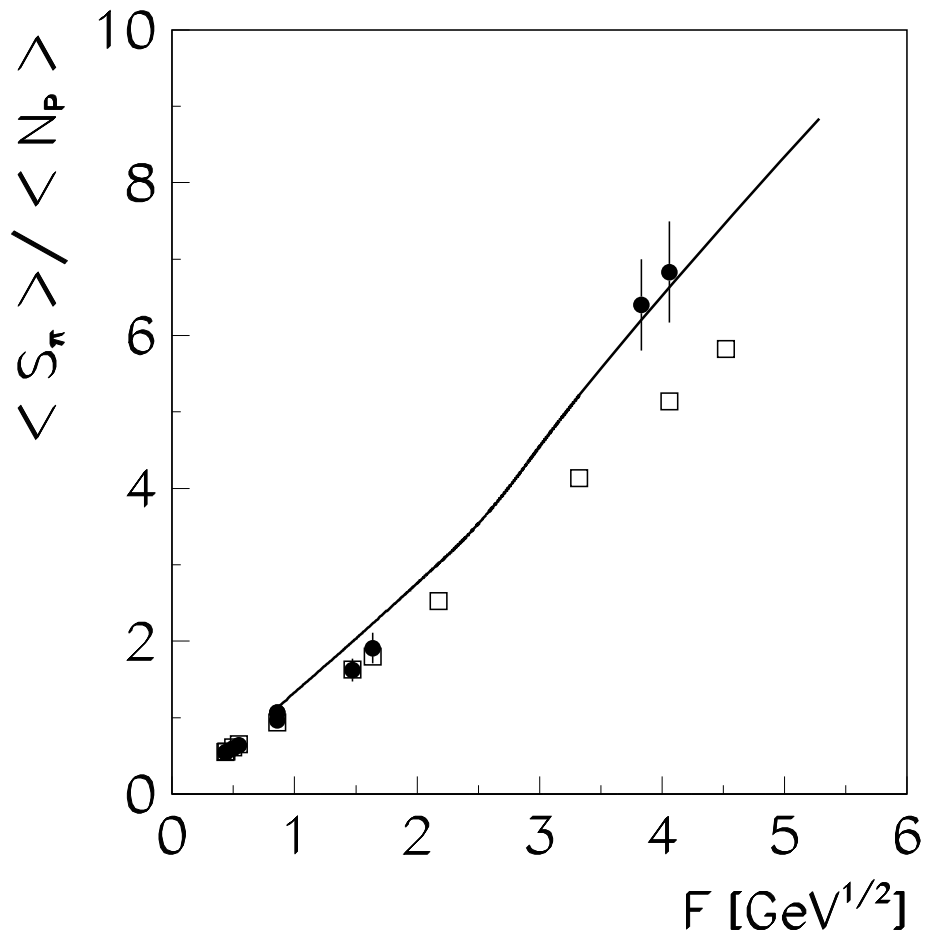


Figure 9: The $\langle S_\pi \rangle / \langle N_P \rangle$ ratio as a function F . Experimental data on central collisions of two identical nuclei are indicated by closed circles. These data should be compared with the model predictions shown by the solid line. The open boxes show results obtained for nucleon–nucleon interactions.

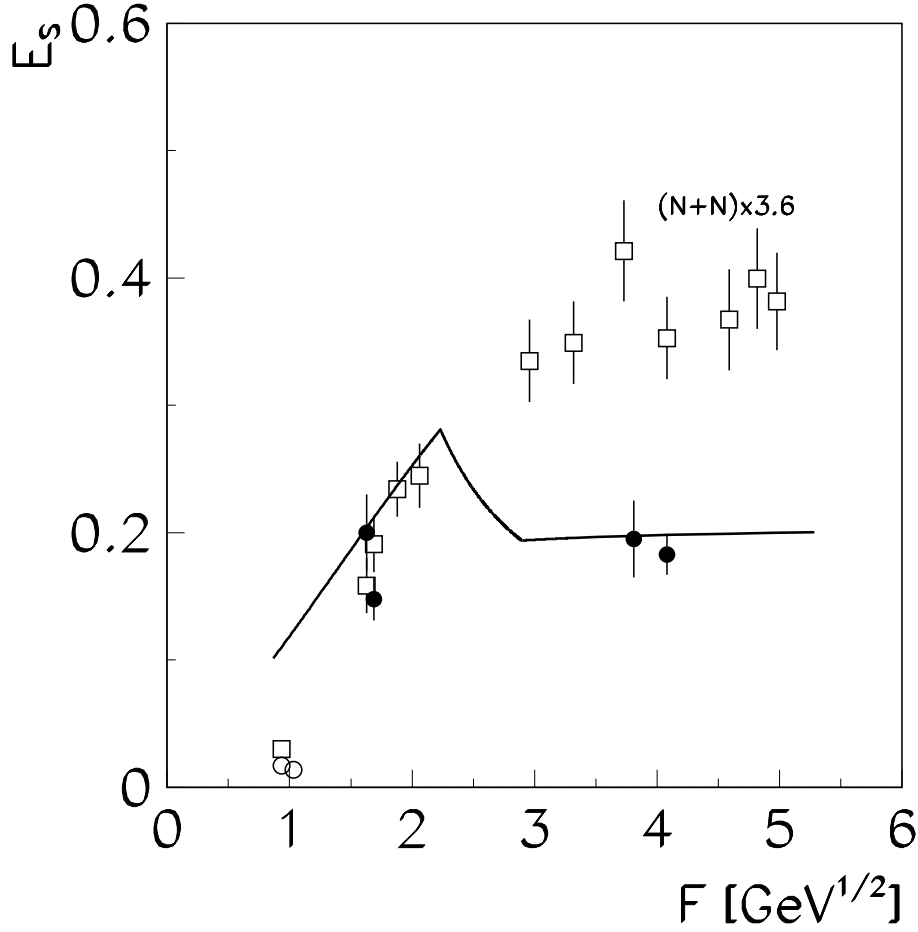


Figure 10: The ratio E_S as a function F . Experimental data on central collisions of two identical nuclei are indicated by closed circles. These data should be compared with the model predictions shown by the solid line. Open circles indicate the results on A+A collisions for which the grand canonical approximation is insufficient. The open boxes show results obtained for nucleon-nucleon interaction, scaled by a factor 3.6 to match A+A data at AGS energy.

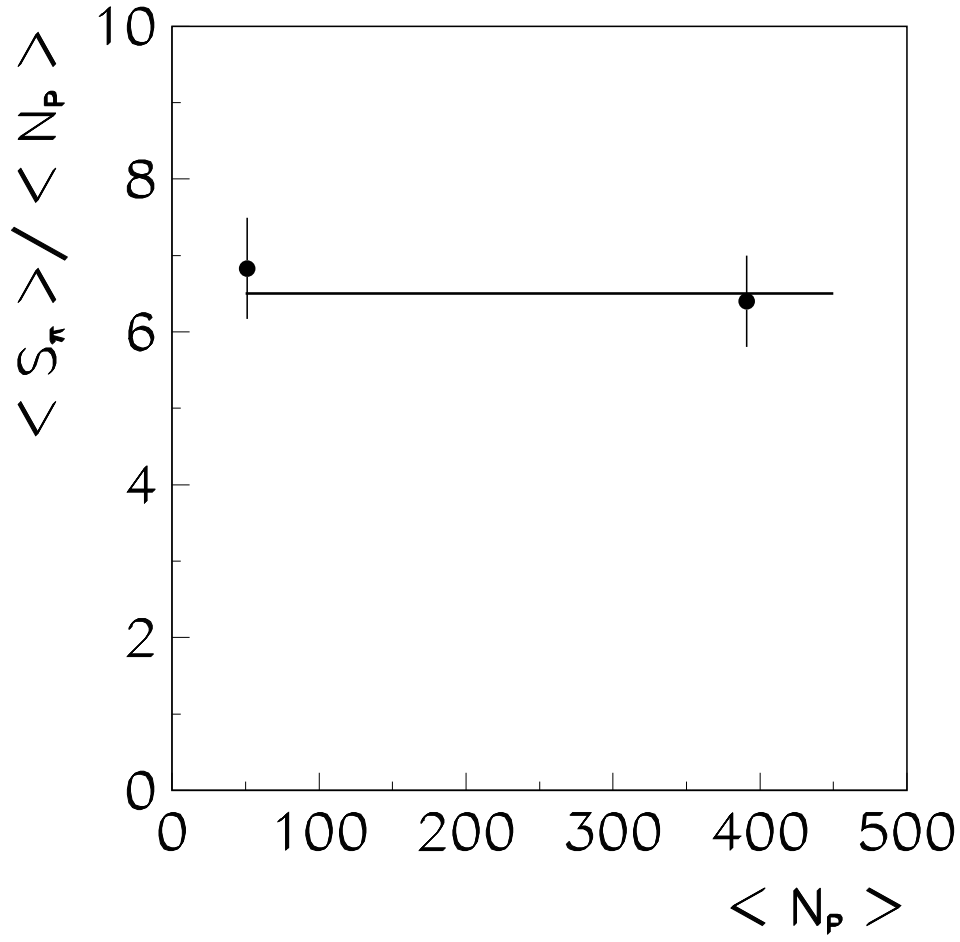


Figure 11: The $\langle S_\pi \rangle / \langle N_P \rangle$ ratio as a function $\langle N_P \rangle$ for central S+S and Pb+Pb collisions at 200 A·GeV and 158 A·GeV. The results are not corrected for a small difference in the collision energy (see Fig. 9). The model prediction is shown by the solid line.

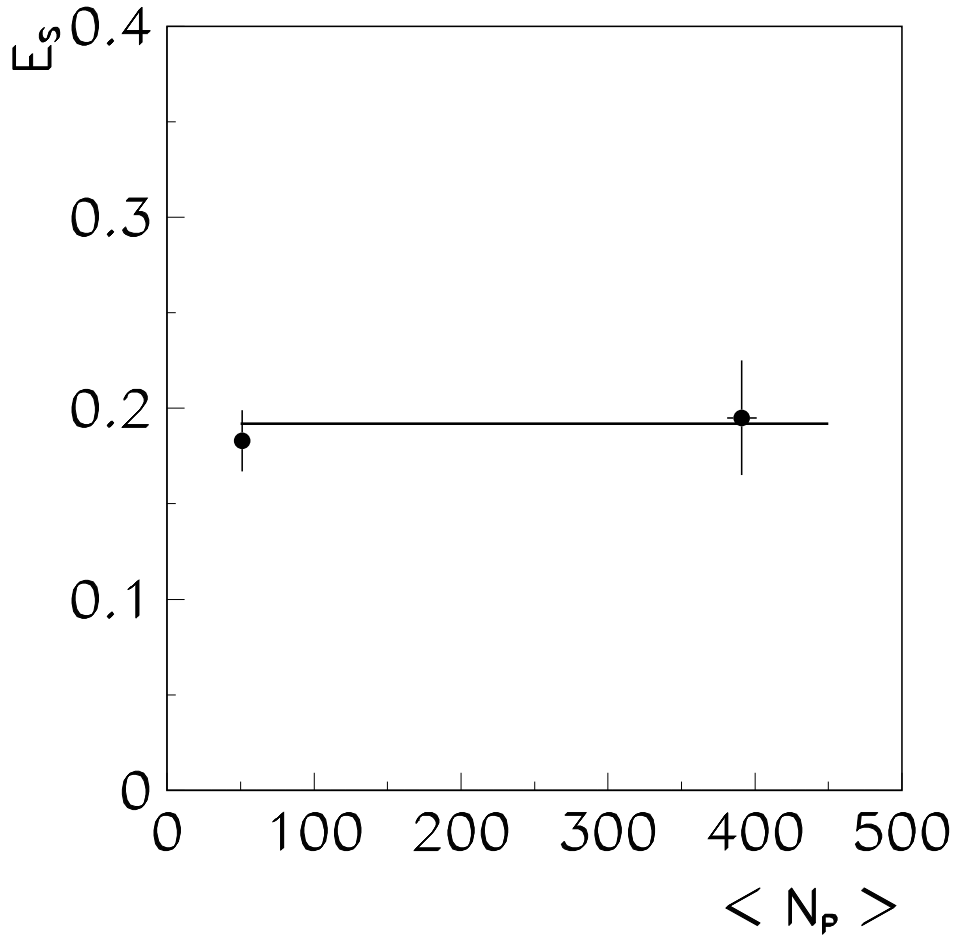


Figure 12: The ratio E_S as a function $\langle N_P \rangle$ for central S+S and Pb+Pb collisions at 200 A·GeV and 158 A·GeV. The results are not corrected for a small difference in the collision energy (see Fig. 10). The model prediction is shown by the solid line.

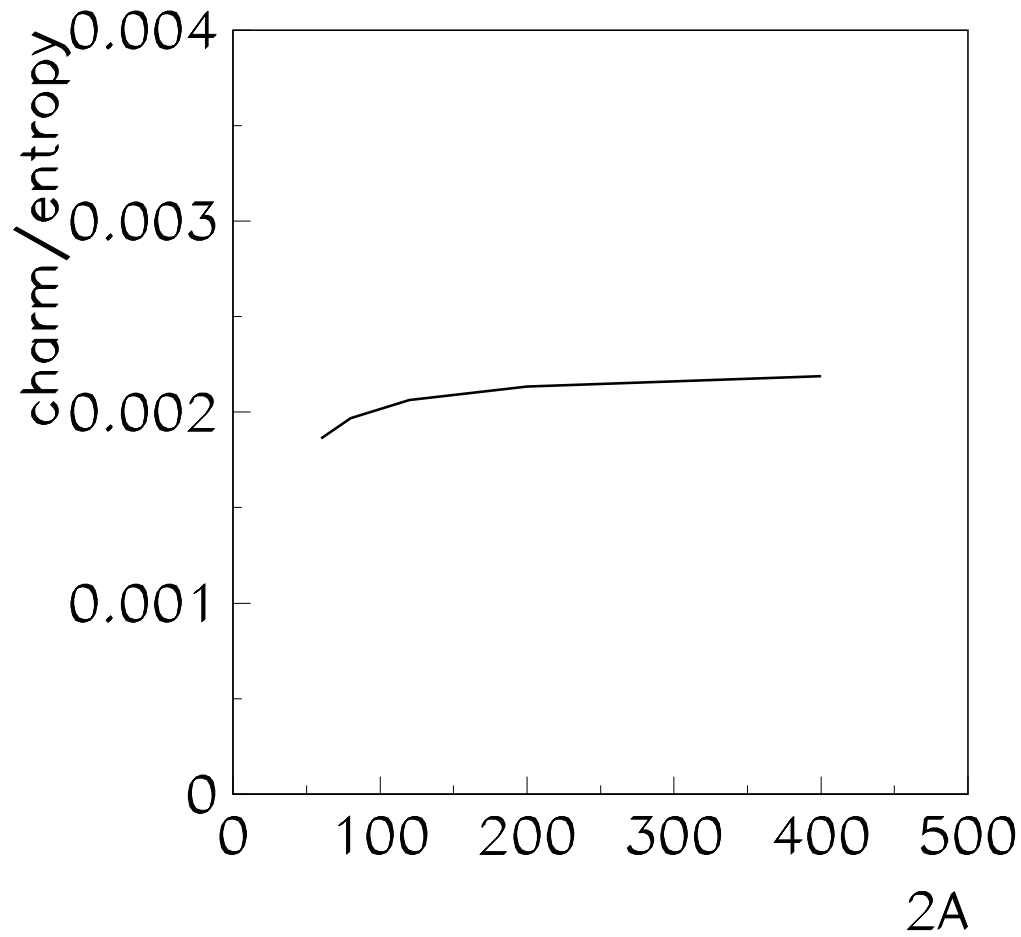


Figure 13: The ratio of charm to entropy as a function of the the number of participant nucleons ($2A$) for A+A collisions at 158 A·GeV. The canonical suppression factor is included in the calculation.

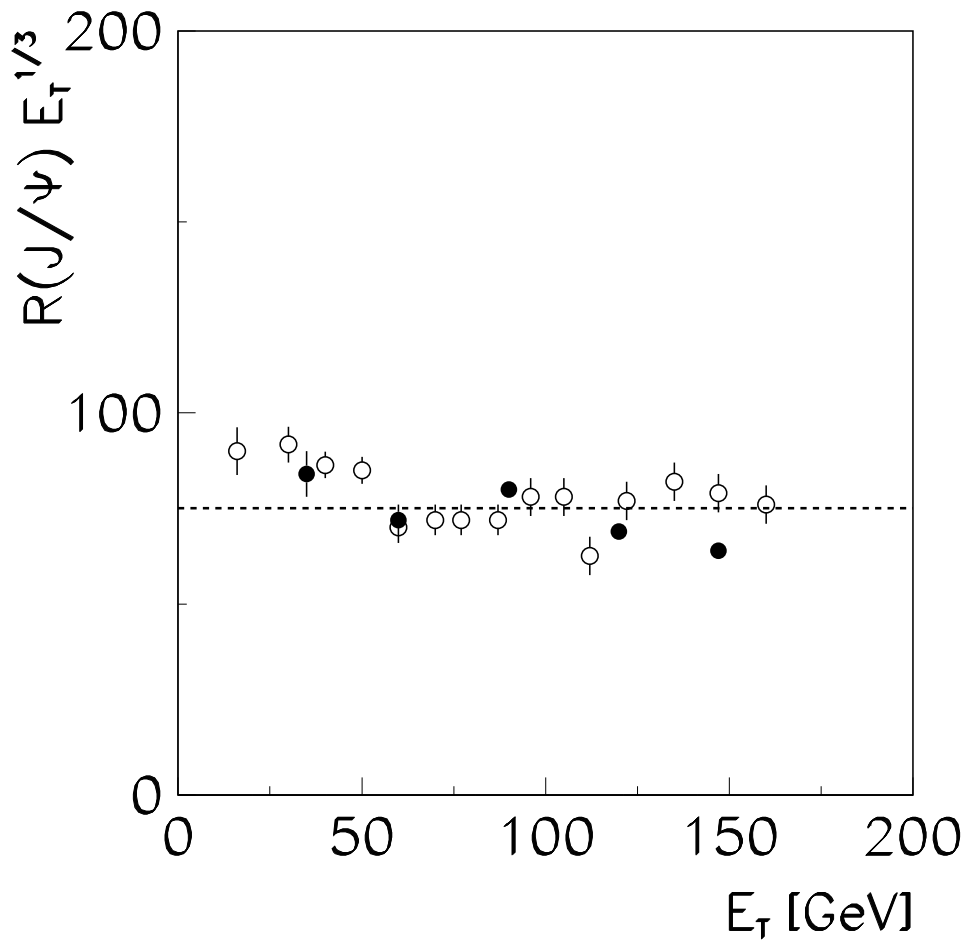


Figure 14: The estimate of the transverse energy dependence of the J/Ψ multiplicity per pion in collisions at 158 A·GeV. The closed points show final 1995 data and the open points preliminary 1996 data of the NA50 Collaboration.